Cross sections for low-energy inelastic H+Li collisions

Andrey K. Belyaev*
Department of Theoretical Physics, A. I. Herzen University, St. Petersburg 191186, Russia

Paul S. Barklem†
Department of Astronomy and Space Physics, Uppsala University, Box 515 SE 751 20 Uppsala, Sweden
(Received 23 June 2003; revised manuscript received 11 August 2003; published 15 December 2003)

We report calculations for the low-energy near-threshold inelastic collision cross sections between the $\mathrm{Li}(2s,2p,3s,3p)+\mathrm{H}(1s)$ states. Results are obtained by solving the coupled-channel equations. Order-of-magnitude estimates for higher states have been made with the multichannel Landau-Zener model. Potentials and couplings from H. Croft *et al* [J. Phys. B **32**, 81 (1999)] are employed. The calculated cross sections are much smaller than ones predicted by the classical Thomsom atom formula currently employed in astrophysics. This result is important for the interpretation of stellar spectra.

DOI: 10.1103/PhysRevA.68.062703 PACS number(s): 34.50.Fa

I. INTRODUCTION

Abundances of the chemical elements in stellar atmospheres are a key observational parameter in understanding the universe. They provide clues about nucleosynthesis, stellar evolution, and mixing processes, and are tracers in galaxy formation and evolution, to name just a few examples. The determination of these abundances is based on the interpretation of absorption lines observed in high resolution spectra, and thus the equation of state of the gas in the stellar atmosphere in which the spectrum is formed.

The efficiency of inelastic collision processes determines if local thermodynamic equilibrium (LTE) is valid, and thus if the Boltzmann distribution adequately describes the atomic energy level populations. If one cannot assume LTE then the atomic energy level populations forming the stellar spectrum are determined by the rates of population and depopulation of the energy levels by radiative and collisional processes (a so-called non-LTE problem). In the atmospheres of hot stars (roughly >7500 K) where hydrogen is ionized, the collisional processes are dominated by electrons. However, in cooler stellar atmospheres collisions with neutral hydrogen atoms may be significant as they outnumber electrons by typically four orders of magnitude. If electron collisions alone are not sufficient to establish thermodynamic equilibrium, it is important to determine the effect of the collisions with hydrogen. For such cool stars where $kT \approx 0.2$–0.6 eV it is the low-energy collisions at and just above the threshold which are of importance in determining the rate coefficient.

The abundance of Li is of particular significance. Since Li was produced in the Big Bang its abundance in the most metal-poor dwarf stars, which presumably preserve the chemical composition of the interstellar gas in the early universe, is an important constraint for models of Big Bang nucleosynthesis, and may be used to constrain the baryon density of the universe. Furthermore, since Li is destroyed at relatively low temperatures, it is a very important probe of mixing processes during stellar evolution.

Steenbock and Holweger [1] first pointed out the possible importance of inelastic collisions with hydrogen in the thermalizing of Li, particularly in metal-poor dwarfs. They estimated the collisional excitation rates for $X+\mathrm{H}$ by modifying a formula from Drawin [2] for H+H which is itself a modification of the classical Thomson formula for excitation by electrons (cf. [3]). In recent years some progress has been made for the H+Na system. Low-energy experimental data have been obtained [4] and calculations performed down to the threshold [5]. However, these results are for only the very lowest states of this one system. For statistical equilibrium calculations, estimates are required for transitions between all states which might affect the population of the states of interest. It is for this reason that the modified Drawin formula is still in use amongst the astrophysics community despite that it is known to overestimate the $\mathrm{H}+\mathrm{Na}(3s)\rightarrow\mathrm{H}+\mathrm{Na}(3p)$ collision rate by several orders of magnitude [5].

In this paper we present quantum dynamical calculations for the H+Li low-energy inelastic cross sections between low-lying states. The calculations are of high accuracy at the threshold. For higher states up to and including the ionic limit we have obtained estimates using the Landau-Zener model, noting that order-of-magnitude estimates will be sufficient to determine if the process is important astrophysically. Interpreted together, these data provide a coherent picture of the excitation, ion-ion neutralization, and ion-pair formation for Li+H and $\mathrm{Li}^+ + \mathrm{H}^-$ collisions required for non-LTE modeling of Li in stellar atmospheres.

II. THEORY

The present quantum treatment of a collision process employs the most widely used approach in atomic collision theory based on the Born-Oppenheimer separation of the electronic and nuclear motion [6], that is, the so-called standard adiabatic approach in an adiabatic representation. The general description of the standard adiabatic approach is discussed in Refs. [7–10] (and references therein), so the method used in the present work is only briefly outlined below.

After the separation of the kinetic-energy operator for the

*Email address: andrey.belyaev@ch.tum.de
†Email address: barklem@astro.uu.se

center of mass of the entire system, the Hamiltonian for a diatomic molecule can be written in the form

$$H=-\frac{\hbar^2}{2M}\frac{\partial^2}{\partial\mathbf{R}^2}+H_{el}(\mathbf{r},\mathbf{R}), \tag{1}$$

where $M=M_AM_B/(M_A+M_B)$ is the reduced mass of the nuclei A and B with corresponding masses M_A and M_B, $\mathbf{R}$ is the vector connecting the nuclei, $\mathbf{r}$ denotes the set of the electronic coordinates measured from the center of nuclear mass, and $H_{el}(\mathbf{r},\mathbf{R})$ is the so-called electronic Hamiltonian, which contains operators of the kinetic energy for the electrons and all interactions. The mass-polarization terms are neglected. The electronic Hamiltonian parametrically depends on $\mathbf{R}$, and its eigenstates form the fixed-nuclei adiabatic electronic basis states $|j\rangle$

$$H_{el}(\mathbf{r},\mathbf{R})\phi_j(\mathbf{r},\mathbf{R})=V_j(R)\phi_j(\mathbf{r},\mathbf{R}) \tag{2}$$

with the eigenfunctions $\langle\mathbf{r}|j\rangle=\phi_j(\mathbf{r},\mathbf{R})$ and the adiabatic potential energies $V_j(R)$.

The wave function for the total system Ψ can be written as a sum of terms $\Psi_{JM_J}(\mathbf{r},\mathbf{R})$ characterized by the total angular momentum quantum numbers J and M_J ($M_J\geqslant 0$). If the theoretical treatment can be restricted to Σ states only (in particular, the rotational couplings are neglected), which is the case at low collision energies E for the process in question, then each wave function $\Psi_{JM_J}(\mathbf{r},\mathbf{R})$ can be expanded as

$$\Psi_{JM_J}(\mathbf{r},\mathbf{R})=Y_{JM_J}(\Theta,\Phi)\sum_j\frac{F_j(R)}{R}\phi_j(\mathbf{r},\mathbf{R}). \tag{3}$$

Y_{JM_J} are the spherical harmonics, where Θ and Φ are the spherical coordinate angles of the vector $\mathbf{R}$. The functions $F_j(R)$ describe the radial motion of the nuclei. Substituting the expansion (3) into the stationary Schrödinger equation $(H-E_{tot})\Psi_{JM_J}=0$ [$E_{tot}=E+V_{in}(\infty)$ being the total energy], multiplying it by $\phi_k^*(\mathbf{r},\mathbf{R})$, and integrating over the electronic coordinates, one obtains a set of coupled channel equations in the adiabatic representation [8,10]

$$\left[-\frac{\hbar^2}{2M}\frac{d^2}{dR^2}+V_j(R)+\frac{\hbar^2}{2M}\frac{J(J+1)}{R^2}-E_{tot}\right]F_j(R)$$
$$=\frac{\hbar^2}{M}\sum_k\langle j|\frac{\partial}{\partial R}|k\rangle\frac{dF_k(R)}{dR}+\frac{\hbar^2}{2M}\sum_k\langle j|\frac{\partial^2}{\partial R^2}|k\rangle F_k(R). \tag{4}$$

The adiabatic potentials and first derivative nonadiabatic matrix elements are usually calculated by quantum chemical programs. The double derivative couplings are not usually calculated explicitly. In the adiabatic basis they cannot be neglected entirely, as they are required for current conservation. They are modeled by setting [5]

$$\langle j|\frac{\partial^2}{\partial R^2}|k\rangle=\frac{d}{dR}\langle j|\frac{\partial}{\partial R}|k\rangle. \tag{5}$$

In order to calculate the scattering matrix and then transition probabilities, cross sections, and rate constants, one needs to solve the coupled channel equations (4) with proper boundary conditions. The boundary conditions are set in two parts: at $R\to 0$ and at $R\to\infty$. At $R\to 0$ the solutions of the coupled equations must obey the boundary conditions:

$$F_j(R)\to 0 \quad \text{as} \quad R\to 0. \tag{6}$$

The boundary conditions for the total (electronic and nuclear) wave function in the asymptotic ($R\to\infty$) region reads

$$\Psi_{JM_J}(\mathbf{r},\mathbf{R})=\sum_j K_j^{-1/2}(a_j^+\Psi_j^++a_j^-\Psi_j^-), \tag{7}$$

with $K_j=\sqrt{2M[E-V_j(\infty)]}/\hbar$ being the channel wave numbers, $a_j^\pm$ being the amplitudes of the incoming and outgoing currents for the channel j, and

$$\Psi_j^\pm=\frac{\exp(\pm iK_jR_j)}{R_j}Y_{JM_J}(\Theta,\Phi)\phi_j \tag{8}$$

being the incoming and outgoing asymptotic wave functions. The vector $\mathbf{R}_j$ connects the centers of mass of the atoms, in contrast to $\mathbf{R}$, which connects the nuclei

$$\mathbf{R}_j=\mathbf{R}+\gamma_j\frac{m_j}{M}(\mathbf{r}-\gamma_j\mathbf{R}). \tag{9}$$

The scalar factors γ_j depend on with which nucleus the electrons travel in the asymptotic region and are defined by

$$\gamma_j=\begin{cases}-\dfrac{M_B}{M_A+M_B} & \text{electron traveling with nucleus } A\\ +\dfrac{M_A}{M_A+M_B} & \text{electron traveling with nucleus } B.\end{cases} \tag{10}$$

m_j is the reduced mass of the electron (bound to a corresponding atom) in the channel j: $m_j=m_eM_A/(m_e+M_A)$, if the electron is bound to nucleus A, and $m_j=m_eM_B/(m_e+M_B)$, if the electron is bound to nucleus B; m_e being the electron mass. Comparison of Eqs. (3) and (7) gives the following form for the radial wave functions:

$$F_j(R)=\sum_k K_k^{-1/2}[a_k^+t_{jk}^+\exp(iK_kR)$$
$$+a_k^-t_{jk}^-\exp(-iK_kR)] \quad \text{for} \quad R\to\infty, \tag{11}$$

where the elements of the matrices $\underline{\underline{t}}^-$ and $\underline{\underline{t}}^+$ represent the reprojection coefficients between the incoming and the outgoing correct asymptotic wave functions and the incoming and the outgoing asymptotic functions of the homogeneous coupled channel equations. At low collision energies these

matrix elements can be evaluated via the corresponding atomic dipole moment matrix elements [8,9]:

$$t_{kj}^{\pm}=\delta_{kj}\pm iK_j\gamma_j\frac{m}{M}\langle k|z^{at}|j\rangle|_{R\to\infty}, \tag{12}$$

where z^{at} is the projection of the active electron coordinate onto the molecular axis. The $t^{\pm}$ matrices mix the channel radial wave functions in order to achieve the boundary conditions at $R\to\infty$ and, hence, obtain the correct asymptotic incoming and outgoing wave functions from the solutions of the coupled channel equations.

On the other hand, radial nonadiabatic coupling matrix elements also correspond to the same atomic dipole moment matrix elements. The point is that the derivative coupling matrix elements used in the coupled equations (4) should be calculated with the origin of the electron coordinates $\mathbf{r}$ at the center of mass of the nuclei. In these coordinates, the orbital wave functions for the active electron in the asymptotic region take the form

$$\langle\mathbf{r}|j\rangle=\phi_j(\mathbf{r}-\gamma_j\mathbf{R}) \quad \text{as} \quad R\to\infty. \tag{13}$$

As a consequence, the $\langle j|\partial/\partial R|k\rangle$ do not automatically go to zero at infinity. It can be shown [8–10] that their asymptotic values are equal to

$$\langle j|\frac{\partial}{\partial R}|k\rangle=\gamma_k\frac{m}{\hbar^2}(V_j-V_k)\langle j|z^{at}|k\rangle\Big|_{R\to\infty}. \tag{14}$$

Finally, for nondegenerate states and low collision energies the $t^{\pm}$ matrix elements can be evaluated via the potentials and the nonadiabatic couplings calculated in the Jacobi coordinates where electron coordinates are measured from the center of nuclear mass

$$t_{kj}^{\pm}=\delta_{kj}\pm\frac{iK_j\hbar^2}{M(V_k-V_j)}\ \langle k|\frac{\partial}{\partial R}|j\rangle\Big|_{R\to\infty}. \tag{15}$$

It is seen that the elements of the $t^{\pm}$ matrices are energy dependent. In the zero-energy limit the $t^{\pm}$ matrices become the unit matrix, which allows one to neglect the electron translation effect at ultralow energies.

The scattering matrix $\underline{S}$ is defined by the relation between the incoming and the outgoing channel amplitudes

$$\underline{a}^{+}=(-1)^{J+1}\underline{\underline{S}}\ \underline{a}^{-}, \tag{16}$$

where $\underline{a}^{\pm}$ denote the column vectors constructed from the corresponding amplitudes. If the solution of the coupled equations is presented by the matrix $\underline{\underline{R}}$ at the (infinitely) large internuclear distance R_0

$$\underline{F}=\underline{\underline{R}}\ \underline{F}', \tag{17}$$

then Eq. (11) allows one to calculate the scattering matrix by means of the following formula [8,9]:

$$\underline{\underline{S}}=(-1)^J\exp(-i\underline{\underline{K}}R_0)\underline{\underline{K}}^{1/2}(\underline{\underline{t}}^{+}-i\underline{\underline{R}}\ \underline{\underline{t}}^{+}\underline{\underline{K}})^{-1}\times(\underline{\underline{t}}^{-}+i\underline{\underline{R}}\underline{\underline{t}}^{-}\underline{\underline{K}})\underline{\underline{K}}^{-1/2}\exp(-i\underline{\underline{K}}R_0), \tag{18}$$

where the elements of the matrices $\underline{K}$, $\underline{K}^{1/2}$ and $\exp(-i\underline{K}R_0)$ are the channel wave numbers, the square roots of these wave numbers, and the corresponding exponents, respectively.

In the practical implementation of the *S*-matrix calculations numerical integration can be reduced by using the WKB approximation, that is, the coupled equations (4) should be solved numerically between a small (zero) distance and a large (but finite) value $R_{end}<R_0$, where all nonadiabatic couplings and potentials V_j are sufficiently constant. The properties of the numerical solution are expressed by the *R* matrix at R_{end} and the *S* matrix is then computed as follows:

$$\underline{\underline{S}}=(-1)^J\exp(-i\underline{\underline{\Phi}})\underline{\underline{\kappa}}^{1/2}(\underline{\underline{\tau}}^{+}-i\underline{\underline{R}}\underline{\underline{\tau}}^{+}\underline{\underline{\kappa}})^{-1}\times(\underline{\underline{\tau}}^{-}+i\underline{\underline{R}}\underline{\underline{\tau}}^{-}\underline{\underline{\kappa}})\underline{\underline{\kappa}}^{-1/2}\exp(-i\underline{\underline{\Phi}}), \tag{19}$$

where the diagonal matrices $\underline{\underline{\kappa}}$ and $\exp(-i\underline{\underline{\Phi}})$, respectively, consist of the local wave numbers

$$\kappa_j(R)=\sqrt{\frac{2M}{\hbar^2}[E_{tot}-V_j(R)]-\frac{J(J+1)}{R^2}} \tag{20}$$

and the elements $\exp(-i\Phi_j)$ are the usual WKB phases of $\Phi_j(R)$. The $\tau^{\pm}$-matrices have the same meaning as the $t^{\pm}$ matrices, but at the smaller internuclear distance R_{end}. Their elements are defined

$$\tau_{kj}^{\pm}(R)=\delta_{kj}\pm\frac{i\kappa_j(R)\hbar^2}{M[V_k(R)-V_j(R)]}\langle k|\frac{\partial}{\partial R}|j\rangle. \tag{21}$$

The values of these quantities must be taken at $R=R_{end}$.

The background of the relation (19) is that one has to mix the computed radial functions $F_j(R)$ in order to account correctly for the electron translation effects in the asymptotic wave functions [8,9]. This is done via the matrices $\underline{\tau}^{\pm}$. When the matrices $\underline{\tau}^{\pm}$ are replaced by the unit matrix, Eq. (19) becomes the usual relation between *R* and *S* matrices, which is valid in the absence of asymptotic couplings. Equation (19) is further based on the construction of a WKB-type solution to the coupled equations beyond R_{end}. The WKB approximation is important only for computational convenience. It might be removed by extending the numerical calculation to a distance, which is so large that not only variations of both the adiabatic potentials and couplings, but also the centrifugal potentials are negligible.

Once the scattering matrix is known, the nonadiabatic transition probabilities can be then calculated from the corresponding *S*-matrix elements

$$P_{jk}=|S_{jk}|^2. \tag{22}$$

Except for very low energies, a large number of *J* values contribute to the cross sections, giving *J* the character of a quasicontinuous variable. In this case, the quantum number *J* can be replaced by the impact parameter *b*, defined as

$$b=\sqrt{\frac{J(J+1)}{2ME}}, \tag{23}$$

and the cross sections can be computed as integrals over the impact parameter

$$\sigma_{jk}(E) = 2\pi p_j^{stat} \int_0^\infty P_{jk}(b,E) b db, \tag{24}$$

where $p_j^{stat} = 1/g_j$ is the statistical probability for population of the initial channel j (g_j being the statistical weight of the channel).

Thus, the standard adiabatic approach allows one to perform a theoretical study of a collision process into two steps: (i) to calculate the adiabatic potential energies and the nonadiabatic couplings in the fixed-nuclei approximation (the so-called quantum chemical part) and (ii) to treat the nuclear motion by solving the coupled channel equations (4) making use of the quantum chemical data calculated in the first step.

It should be noted that besides the method described above there are other methods treating collision processes within or beyond the standard adiabatic approach. The former are typically based on the inclusion of electron or common translation factors, see Ref. [11] for a review, references, and applications to the $He^{2+}+H$ collision test case. An example of the latter is the hyperspherical close-coupling method recently described and applied to the same test case in Ref. [12]. A discussion of these methods is outside the score of the present paper, but it is interesting to note that the results of the different methods agree well with each other in the energy range roughly between 100 eV and 1 keV, while discrepancies were found at both low and high energies.

III. QUANTUM CHEMICAL DATA

In this work we study low-energy Li+H collisions and, hence, neglect rotational couplings and consider only the $^1\Sigma^+$ states of the LiH system. We therefore require the adiabatic $^1\Sigma^+$ potentials $V_j(R)$ and radial couplings between $^1\Sigma^+$ states $\langle j|\partial/\partial R|k\rangle$, as input for the coupled channel equations (4). The LiH system has been quite extensively investigated, e.g., Refs. [13–15]. The LiH $^1\Sigma^+$ adiabatic potentials show a series of avoided crossings between covalent states and the ionic state $H^- + Li^+$, as seen in other alkali-hydrides (e.g., [16,17]). Previous work [4,5] has demonstrated that for lower states of the H+Na system, at low-energy these crossings between the ionic and covalent states represent the most important mechanism in the inelastic process in question.

In this work we use the adiabatic potential data for the singlet system of [15] which is an improved version of the data from [13,14]. The radial couplings were computed by us by direct numerical differentiation (see [14]) of the the C_{jk} matrices provided to us by these authors. As the quantum chemical data of [15] do not include data for separations smaller than $R=2$ a.u., we have performed additional calculations of the adiabatic potentials and the radial nonadiabatic couplings for the low-lying LiH($^1\Sigma^+$) states using the MOLPRO code [18], to estimate these at very short internuclear distance.

The quantum chemical data relevant to the excitation process treated are shown in Fig. 1. The adiabatic potentials for the LiH($^1\Sigma^+$) states are plotted in Fig. 1(a), while the radial nonadiabatic couplings are shown in Figs. 1(b) and 1(c). It should be pointed out that due to the method used in the quantum chemical calculations in [15] all nonadiabatic couplings asymptotically ($R\to\infty$) go to zero, although some of them must have nonvanishing values at infinity, see Eq. (14). Estimates made in the present work show that nonvanishing values are small, and as the collision energies treated are low ($E\leqslant 10$ eV), the neglection of the electron translation effects gives an uncertainty not more than a couple of percent in the cross sections.

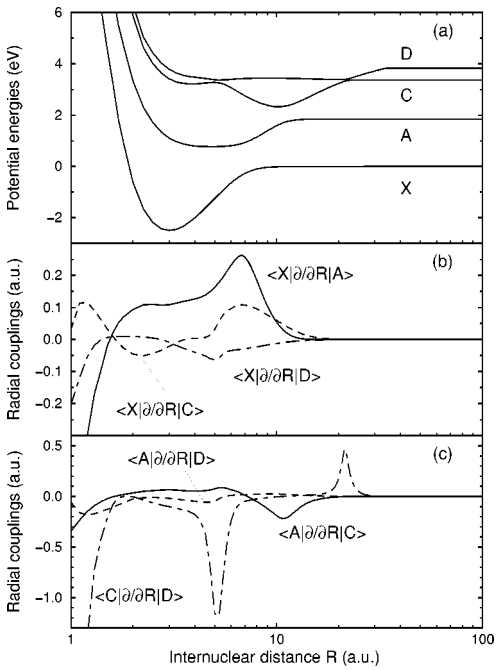

FIG. 1. Quantum chemical data for the LiH($^1\Sigma^+$) quasimolecule. (a) The adiabatic potentials for the four lowest $^1\Sigma^+$ states; (b) and (c), the nonadiabatic radial coupling matrix elements $\langle j|\partial/\partial R|k\rangle$ between the states.

Figure 1(a) shows that there are a number of nonadiabatic regions. The most important for the excitation processes under consideration are: at the internuclear distances $R\approx 6.75$ a.u. between the $X\ ^1\Sigma^+$ and $A\ ^1\Sigma^+$ molecular states; at $R\approx 10.75$ a.u. between the $A\ ^1\Sigma^+$ and $C\ ^1\Sigma^+$ states; at $R\approx 21.5$ a.u. between the $C\ ^1\Sigma^+$ and $D\ ^1\Sigma^+$ states. At these distances the adiabatic potentials indicate avoided crossings. Indeed the radial coupling matrix elements $\langle j|\partial/\partial R|k\rangle$ depicted in Figs. 1(b) and 1(c) show peaks at the same distances confirming the avoided crossing interpretation. The area under each of the peaks is close to $\pi/2$, and the situation is expected to correspond closely to the Landau-Zener model. These crossings appear due to interactions of the ionic $H^- + Li^+$ state with the covalent states, the situation typical for alkali-hydrides (see, e.g., [4,5,13–17]). In addition to the above mentioned avoided crossings there are some extra nonadiabatic regions, for example, at $R\approx 0.775$ a.u. between the $X\ ^1\Sigma^+$ and $A\ ^1\Sigma^+$ states, at $R\approx 5.25$ a.u. and $R\approx 1.0$ a.u. between $C\ ^1\Sigma^+$ and $D\ ^1\Sigma^+$. They also affect the nuclear dynamics mainly by redistributing the cur-

rents between molecular states leading, for instance, to Rosenthal oscillations.

IV. QUANTUM DYNAMICAL CALCULATIONS

The program used in the present work for numerical integration of the coupled channel equations (4) is described in Ref. [5]. In the present work the numerical calculations were carried out with a four-state basis for the singlet system (the molecular states $X\ ^1\Sigma^+$, $A\ ^1\Sigma^+$, $C\ ^1\Sigma^+$, and $D\ ^1\Sigma^+$ asymptotically correlated to the $H+Li(2s,2p,3s,3p)$ atomic states) for the collision energies from the energy threshold till 10 eV.

The choice to restrict the calculations to the four-state basis has the following justification. Firstly, for collisions of the atoms in their ground states at collision energies near the $Li(2p)$ excitation threshold there are only two open channels, so even a two-state basis is sufficient. At higher, but still low energies the $H+Li(3s,3p)$ channels become open and the four-state basis is sufficient for the study of the $Li(2p)$ and $Li(3s)$ state excitation near threshold. Extension of the basis does not change the nonadiabatic transition probabilities from the ground state to the two nearest states.

Secondly, as will be shown, the nonadiabatic transitions between the lowest-lying states must be treated quantum mechanically, while other transitions can be treated in the framework of the Landau-Zener model. Although the nonadiabatic regions between the low-lying states have an area under the nonadiabatic coupling function close to $\pi/2$ and thus might be expected to be close to the Landau-Zener case, other features (like broad, dense, and overlapping nonadiabatic regions, Rosenthal oscillations, grazing incidence, etc.) affect the nonadiabatic transitions between the low-lying states. The transitions between the states higher than and including the $H+Li(3p)$ state can be treated by means of the Landau-Zener model since the nonadiabatic regions are better localized and separated [see Figs. 1(b) and 1(c)], which leads to a situation where the Landau-Zener model prerequisites are better fulfilled, and, hence, the Landau-Zener model gives reasonable estimates. Similar results have been found by [19] for LiH and [20] for the similar NaH system. Thus, the four-state basis is sufficient for an accurate treatment of the nonadiabatic transitions which must be treated quantum mechanically at collision energies near threshold.

Within the four-state approximation used in the present quantum dynamical calculations no excitation of states above $Li(3p)$, including the ionic $Li^+ + H^-$ state, is taken into account, although these states are indeed populated, if the collision energy is high enough. For this reason the result for the population of the $Li(3p)$ state should be in fact redistributed between the $Li(3p)$ and upper states. In this section what is called "the excitation of the $Li(3p)$ state" should be treated as the total excitation of the $Li(3p)$ state and all higher (energetically allowed) states. The redistribution has been estimated by means of a multichannel Landau-Zener model approach (see the Appendix), from which we find that once other channels are open the real $Li(3p)$ excitation is expected to be only a few percent of this total excitation. The Landau-Zener calculations indicate that the system passes

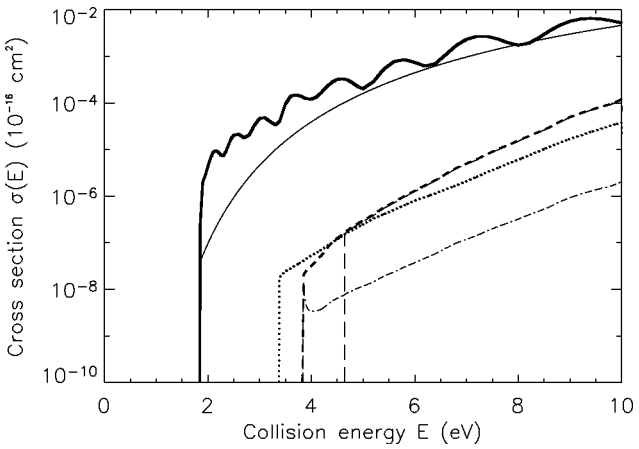

FIG. 2. The calculated cross sections for the excitation process $Li(2s)+H \rightarrow Li(2p,3s,3p)+H$ as a function of the collision energy in the four-state approximation. The thick solid line is the cross section for the excitation of $Li(2p)$; the dotted curve is for $Li(3s)$; and the short-dashed line is for the $Li(3p)$ state. The thin solid line is the cross section for the excitation of $Li(2p)$ from the Landau-Zener model. The dot-dashed and long-dashed lines show the excitation of the $Li(3p)$ and the ionic states respectively, where the quantal $Li(3p)$ result has been redistributed based on the Landau-Zener model estimates.

the higher ionic avoided crossings practically diabatically even at the low energies considered here and thus most of the population is expected to go to the ionic state (when this channel is open), in agreement with [19]. This indicates that the inclusion of higher states would have negligible effect on the results.

It should be also pointed out that all adiabatic potentials are attractive at large internuclear distances, and this results in the appearance of so-called orbital resonances. These resonances were found in the corresponding process for $Na+H$ collisions [5]. Although the resonant peaks are as much as 4 orders of magnitude larger than the nonresonant cross sections, the resonant cross sections are very narrow [5] and, hence, give less than a 10% contribution to the corresponding rate constant. For this reason the orbital resonances are neglected in the present work.

The calculated cross sections for the excitation from the ground $Li(2s)$ state are presented in Fig. 2, for the excitation from the $Li(2p)$ state in Fig. 3, and for the excitation from the $Li(3s)$ state in Fig. 4. In each case the cross sections for population to the $Li(3p)$ state are also shown where the distribution between the $Li(3p)$ and ionic states has been estimated from the Landau-Zener calculations (see the Appendix).

It is seen from Fig. 2 that inelastic $Li(2s)+H$ collisions lead mainly to the excitation of the $Li(2p)$ state, although this cross section is quite small, between 10^{-22} and 10^{-18} cm^2. The $Li(3s)$ and the $Li(3p)$ excitation cross sections are typically 2 to 4 orders of magnitude smaller. The basic mechanism for the $Li(2p)$ excitation is nonadiabatic transitions at the avoided crossing between the $X\ ^1\Sigma^+$ and $A\ ^1\Sigma^+$ states around $R \approx 6.75$ a.u., although the nonadiabatic region around $R \approx 0.775$ a.u. also contributes but affects pre-

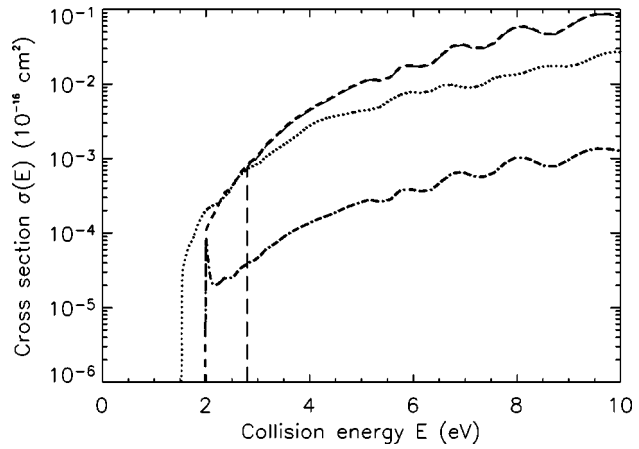

FIG. 3. The calculated cross sections for the excitation process $Li(2p)+H \rightarrow Li(3s,3p)+H$ as a function of the collision energy in the four-state approximation. The dotted line is the cross section for the excitation of $Li(3s)$, while the short-dashed line is for the $Li(3p)$ state. The dot-dash and long-dashed lines show the excitation of the $Li(3p)$ and the ionic states, respectively, where the quantal $Li(3p)$ result has been redistributed based on the Landau-Zener model estimates.

dominantly the oscillations of the cross sections. It has been checked that in the absence of nonadiabatic couplings at $R<2$ a.u. the cross section oscillations are shifted in collision energy, but retain more or less the same average value, though at a particular collision energy the cross section can change by up to a factor of 2. The oscillation of the $Li(2s)-Li(2p)$ excitation cross section is due to the Stückelberg and Rosenthal phases.

In addition to the quantal results, Fig. 2 shows the cross sections for excitation of the $Li(3p)$ state and for population of the ionic H^-+Li^+ state obtained by redistribution of the quantal four-state $Li(3p)$ cross section based on the multichannel Landau-Zener model described in the Appendix. It is seen that the pure $Li(3p)$ population becomes only a few percent of the four-state quantal result for collision energies where the next channel $[H+Li(3d)]$ is open. This result confirms that above and including the $H+Li(3p)$ channel the nonadiabatic regions between the ionic and the covalent diabatic molecular states are passed by the system mainly diabatically, which is in agreement with the previous results from mutual neutralization calculations [15,19]. As the states above the ionic H^-+Li^+ state are not coupled with the ionic state, once the ionic channel becomes open the dominant part of the outgoing current goes into that channel. Thus, the cross section for the ionic state population practically coincides with the quantal four-state cross section for population of the $H+Li(3p)$ channel for the energies above the ionic threshold. At the collision energies between the $H+Li(3p)$ and the ionic state threshold the redistribution of the quantal four-state $Li(3p)$ excitation cross section results in dominant population of the highest energetically allowed state, and this population becomes small as soon as the next channel opens. This result holds for population of the states up to and including the ionic state from other initial channels, see, e.g., Figs. 3 and 4.

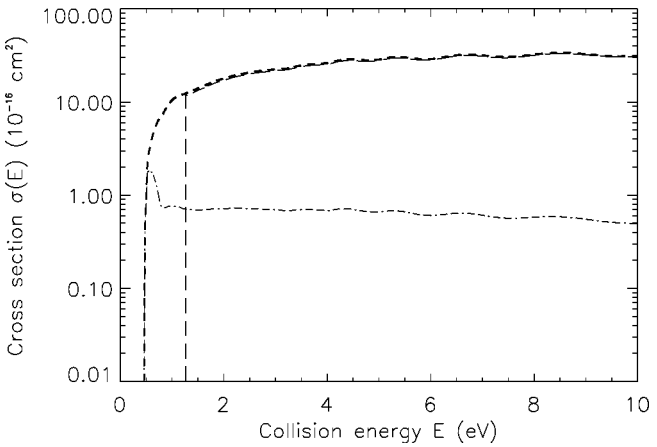

FIG. 4. The calculated cross section (short-dashed line) for the excitation process $Li(3s)+H \rightarrow Li(3p)+H$ as a function of the collision energy in the four-state approximation. The dot-dash and long-dashed lines show the excitation of the $Li(3p)$ and the ionic states, respectively, where the quantal $Li(3p)$ result has been redistributed based on the Landau-Zener model estimates.

The $Li(2p)$-$Li(3s,3p)$ excitation cross sections in Fig. 3 are typically an order of magnitude larger than the $Li(2s)$-$Li(2p)$ results [the $Li(2p)$-$Li(2s)$ deexcitation cross section can be easily calculated from the $Li(2s)$-$Li(2p)$ one]. The basic mechanism here is due to the nonadiabatic region between the $A\ ^1\Sigma^+$ and $C\ ^1\Sigma^+$ states around $R \approx 10.75$ a.u.

$Li(3s)+H$ collisions result in the large $Li(3p)$ excitation cross section (Fig. 4) due to the nonadiabatic regions between $C\ ^1\Sigma^+$ and $D\ ^1\Sigma^+$ states around $R \approx 21.5$ a.u. and $R \approx 5.25$ a.u. Though the potential splittings are small in these regions and the system passes the regions mainly diabatically, the nonadiabatic regions are at large internuclear distances, and hence a wide range of impact parameters contribute to the cross section. But again only a small fraction of this population really goes to the $Li(3p)$ state, while the main part of the outgoing current goes to the ionic state.

A comparison of the four-state quantal and the multichannel Landau-Zener results shows that the Landau-Zener model fails to describe the nonadiabatic transitions between the ground $H+Li(2s)$ and the $H+Li(2p)$ states at the near-threshold collision energies (see Fig. 2), but provides reasonable results (within an order of magnitude) for transitions between the states higher than and including the $H+Li(2p)$ state. Based on this, as well as the fact that the nonadiabatic regions are better localized for the states higher than $H+Li(3s)$, the multichannel Landau-Zener model is expected to provide reasonable estimates for population of the states above and including the $H+Li(3p)$ channel, including the ionic state.

V. DISCUSSION AND CONCLUSIONS

We calculated the integral cross sections for the electronic excitation of Li atoms by H atom impact for energies between the thresholds and 10 eV by means of the full quantum approach. We have employed $^1\Sigma^+$ potentials and nonadia-

batic radial couplings from the literature [13–15]. It has been shown that in the $^1\Sigma^+$ system for the states up to Li($3p$) the avoided crossing between the ionic and the covalent molecular LiH($^1\Sigma^+$) states is the dominant mechanism for the nonadiabatic transitions.

We will now discuss the accuracy of the calculated cross sections. In general, there are two principal possible origins for uncertainty in the numerical results: The limited precision of the quantum chemical data and the truncation of the basis used in the dynamical treatment, including neglection of rotational couplings and other symmetries (in particular, triplet molecular states).

The accuracy of the quantum chemical data is limited by (i) the precision of the calculated adiabatic potentials, which for modern *ab initio* or pseudopotential calculations is typically believed to be below ± 0.1 eV, (ii) the precision of the single derivative coupling matrix elements, which is believed to be ± 0.01 a.u., and (iii) the use of the approximation in calculation of the double derivative coupling matrix elements [Eq. (5)]. We estimate that the possible uncertainty in the calculated cross sections from these sources does not exceed 50%, 10%, and 10%, respectively. Due to the method used in the quantum chemical calculation it is unlikely that all three of these sources of error contribute strongly to the total error in the calculated cross sections.

The influence of the truncation of the basis set on the accuracy of the calculated cross sections depends on the collision energy and on the chosen initial state. For a given collision energy and initial state the following factors should be discussed: (i) spin symmetry of the molecular states (singlet and triplet states), (ii) symmetry related to the projection quantum number for the electronic orbital angular momentum upon the molecular axis (here only Σ and Π molecular states), and (iii) the number of states of each symmetry taken into account. The error introduced by neglect of certain molecular states can be estimated from the obvious fact that for effective nonadiabatic transitions both a close approach of potentials and a large nonadiabatic coupling are required. Note that rotational couplings enter the coupled channel equation with the factor $1/R^2$ [9], thus, nonadiabatic transitions due to rotational couplings are typically effective at short internuclear distances. The main distinction between the singlet and triplet LiH states is the presence of the strongly attractive ionic ($Li^+ + H^-$) diabatic potential in the singlet system, while such a term is absent in the triplet system. This leads to the series of avoided crossings for the singlet states (see Fig. 1). As mentioned above, this series provides effective nonadiabatic transitions between the low-lying singlet states due to the radial couplings. In addition, the lowest $B\ ^1\Pi$ state [asymptotically corresponding to Li($2p$)+H] is close not to the ground $X\ ^1\Sigma$ state, but to the excited $A\ ^1\Sigma$ state (and even degenerate in the united atom limit), while the lowest triplet $b\ ^3\Pi$ state is close and degenerate in the united atom limit with the $a\ ^3\Sigma$ asymptotically corresponding to Li($2s$)+H. This leads to the fact that for excitation from the ground Li($2s$) state the cross section due to the rotational couplings in the singlet system is one or two orders of magnitude smaller than that due to the radial couplings (except for the orbital resonance cases), while in the triplet system the rotational coupling provides the dominant mechanism, but the corresponding cross section has a significant size only at energies around 10 eV. As the approach of the $a\ ^3\Sigma$ and $b\ ^3\Pi$ states takes place at the highly repulsive part of the potentials, the energy dependence of the $a\ ^3\Sigma \rightarrow b\ ^3\Pi$ cross section is stronger than that of the $X\ ^1\Sigma \rightarrow A\ ^1\Sigma$ cross section. The $a\ ^3\Sigma \rightarrow b\ ^3\Pi$ cross section will be practically zero at the energy threshold, yet similar to the $X\ ^1\Sigma \rightarrow A\ ^1\Sigma$ cross section at around $E=10$ eV. Thus, the neglect of singlet $^1\Pi$ states results in an uncertainty of a few percent for the excitation cross sections in Li($2s$)+H collisions, while the neglect of the triplet system results in practically no error at the energy threshold for the same cross sections, which is the main focus of the present paper, but at the collision energy 10 eV an account of the triplet molecular states can increase the cross sections up to a factor of 2. Thus, as discussed in the preceding section, the size of the present basis is sufficient for Li+H collisions in their ground states near threshold. For collisions of an excited Li atom with hydrogen atoms the situation can be more complicated. Neglect of other symmetries, rotational couplings, and orbital resonances in this work means our results should be a lower limit to the actual cross sections. However, it would be surprising if our results were on average in error by more than a factor of two for Li($2s$)+H collisions, and a factor of three for collisions of excited states (noting that as discussed, results at a given collision energy E may change more substantially).

In summary, it is expected that at the threshold the cross sections are accurate to better than 50%, where the error is dominated by uncertainty in the quantum chemical data. At higher energies, errors due to the limited basis set become important and the total error may be as high as a factor of 3 at 10 eV. However, we emphasize that for the relevant temperatures in the astrophysical problem of interest, the cross sections within 1 eV or so of the threshold dominate.

We found, as in [5] for H+Na low-energy collisions, that the Landau-Zener model fails to quantitatively model excitation from the ground state, particularly at the collision energies treated here where the Landau-Zener $2s \rightarrow 2p$ excitation cross section (between 10^{-24} and 10^{-18} cm^2) is 1–2 orders of magnitude smaller than that calculated by means of the full quantum approach (between 10^{-22} and 10^{-18} cm^2). The modified Drawin formula [1–3] commonly used by the astrophysics community, predicts the $2s \rightarrow 2p$ excitation cross section to be between 10^{-17} and 10^{-15} cm^2 over the same collision energy range, that is, it overestimates the $2s \rightarrow 2p$ excitation cross section by 3 to 5 orders of magnitude as compared with the obtained quantum cross section.

Even this short comparison shows the importance of the quantum calculations of the inelastic cross sections between the low-lying LiH states at low collision energies. On the other hand, as discussed earlier, the Landau-Zener model gives reasonable results for higher states. We have compared results from the multichannel Landau-Zener model calculations with the results here for the more excited states. The results are in reasonable agreement (at least within an order of magnitude) even at the threshold. Order of magnitude estimates are sufficient to determine if this process is important

in stellar atmospheres, and if time and effort should be invested in more detailed calculations. Thus quantum dynamical results obtained in this paper can therefore be complemented by the Landau-Zener model estimations for the excitation cross sections involving higher-lying states below the ionic limit (these results can be obtained from the authors). As we have seen from our Landau-Zener calculations, when open the ionic state is significantly populated. Data from accurate quantum mechanical calculations are already available for this process [15,21]. If necessary the expressions for Rydberg states given by Kaulakys [22] may be used for states above the ionic limit. Together, this information gives the opportunity to model the statistical equilibrium of Li in cool stellar atmospheres, including the effect of inelastic collisions with H. Such modeling has been carried out, and the results along with a complete set of rate coefficients will be published in the astrophysics literature.

ACKNOWLEDGMENTS

We are indebted to F. X. Gadéa and A. S. Dickinson for providing us with the quantum chemical data used in this work. We thank D. Kiselman for suggesting this work. We gratefully acknowledge support from both the Swedish Research Council (VR) and the Swedish Royal Academy of Sciences (KVA). A.K.B. also gratefully acknowledges the partial financial support from the ''Fonds National de la Recherche Scientifique de Belgique'' (FRFC, Belgium) and the program ''Universities of Russia'' No. UR.01.01.006.

APPENDIX: MULTICHANNEL LANDAU-ZENER MODEL

As for the quantum dynamical calculations, we consider only the $^1\Sigma^+$ system, ignoring other symmetries. The ten states up to and including the ionic state are considered, namely those asymptotically correlated to $\mathrm{Li}(2s,2p,3s,3p,3d,4s,4p,4d,4f)+\mathrm{H}(1s)$ and $\mathrm{Li}^+ + \mathrm{H}^-$. Only the nonadiabatic regions at the crossings between the ionic and covalent states are treated, and each crossing is described using the standard Landau-Zener (LZ) model (e.g., [23,24]).

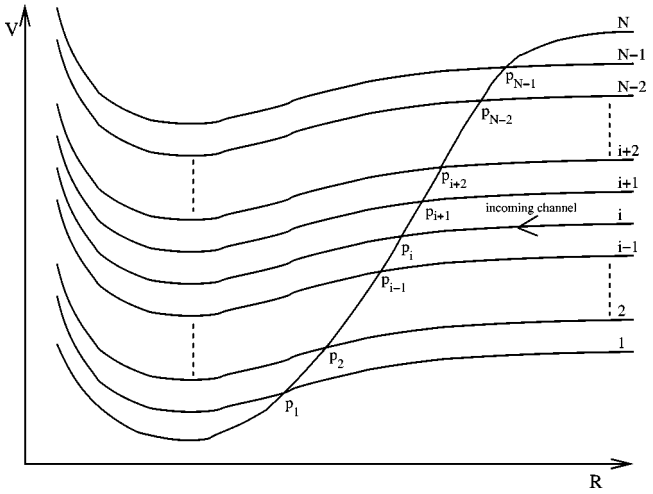

FIG. 5. Schematic diagram of the multichannel Landau-Zener model in the diabatic representation for a series of ionic–covalent crossings.

The generalized multichannel model employed is shown schematically in Fig. 5 in the diabatic representation. It consists of $N-1$ covalent states labeled $1,2,\ldots,N-1$ each crossed by the ionic state N. Nonadiabatic regions are modeled at each curve crossing with a probability p that the system traverses the crossing diabatically (i.e. stays on the same curve) and $1-p$ that the crossing is traversed adiabatically. The probability p is the LZ probability given by

$$p_i(v) = \exp[-2\pi H_{Ni}^2/\hbar v(H'_{NN}-H'_{ii})] \qquad \text{(A1)}$$

where v is the radial velocity of the colliding atoms, and $H_{mn}(R)$ are matrix elements of the electronic Hamiltonian in the diabatic basis as a function of internuclear distance. Primed quantities refer to derivatives with respect to R. All values are evaluated at R_c, the internuclear separation at the crossing.

TABLE I. Landau-Zener model parameters used for the $\mathrm{H}+\mathrm{Li}\,^1\Sigma^+$ system crossings of covalent states i with the ionic state N. Diabatic energies H_{ii} at the crossing are given with respect to the separated atom limit $H_{ii}(\infty)$ which is given relative to the ground state. p_i^{stat} is the statistical probability for population of the initial channel. Note $a(b)=a\times 10^b$.

Covalent state	R_c (a.u)	H_{Ni} (a.u)	$H_{NN}=H_{ii}$ (a.u)	$H'_{NN}-H'_{ii}$ (a.u)	$H_{ii}(\infty)$ (cm^{-1})	p_i^{stat}
$2s$	7.3	0.022	0.014	0.021	0	0.2500
$2p$	11.3	0.011	0.0080	0.0098	14 904	0.0833
$3s$	22.1	0.0011	2.8(−4)	0.0022	27 206	0.2500
$3p$	34.0	2.00(−4)	2.4(−5)	8.70(−4)	30 925	0.0833
$3d$	36.0	5.25(−5)	9.5(−6)	8.20(−4)	31 283	0.0500
$4s$	91.2	1.53(−9)	0	1.10(−4)	35 012	0.2500
$4p$	232.2	1.45(−21)	0	1.76(−5)	36 470	0.0833
$4d$	277.0	2.14(−25)	0	1.30(−5)	36 623	0.0500
$4f$	279.5	1.32(−25)	0	1.27(−5)	36 630	0.0357
ionic					37 405	1.0000

Expressions for the double-passage transition probabilities for the multichannel system have been obtained, essentially rewriting the expressions from [25,26]. For the system with initial channel i, the probability of a final channel f in the deexcitation case where $f<i$ is given by

$$P_{i>f}=2p_f(1-p_i)(1-p_f)\left\{\prod_{l=f+1}^{i-1} p_l\right\} \times\left\{1+\sum_{m=1}^{2(f-1)}\prod_{k=1}^{m}(-p_{f-[(k+1)/2]})\right\}, \quad \text{(A2)}$$

where square brackets [. . .] in the subscript here denotes the largest integer value. For the excitation case $f>i$ the probability is given by

$$P_{i<f}=2p_i(1-p_i)\left\{1+\sum_{m=1}^{2(i-1)}\prod_{k=1}^{m}(-p_{i-[(k+1)/2]})\right\}. \quad \text{(A3)}$$

The probability for the elastic case $f=i$ is given by

$$P_{i=f}=p_i^2+(1-2p_i+p_i^2) \times\left\{1+2\sum_{m=1}^{2(i-1)}\prod_{k=1}^{m}(-p_{i-[(k+1)/2]})\right\}. \quad \text{(A4)}$$

The LZ model parameters for the inner five crossings in the $LiH^1\Sigma^+$ system have been estimated from the adiabatic potential curves of [15]. For outer crossings this is not practical, thus we make the assumption of a practically flat covalent state and a purely Coulombic ionic state and thus estimate $R_c=36.125n_i^{*2}/(18.0625-n_i^{*2})$ and $H'_{NN}-H'_{ii}=1/R_c^2$, where n_i^* is the effective principle quantum number of the Li state in the separated atom limit and results are in atomic units. The behavior with R_c of the diabatic coupling H_{Ni} values derived for the five inner crossings is well fit by an exponential. The H_{Ni} for the outer crossings have been estimated by extrapolation of this fit. The adopted model parameters are given in Table I.

Results have been obtained for this ten state model using the method of partial waves (e.g., [23,27]). In order to make meaningful comparisons with the results of the quantum dynamical calculation we have also computed results in the four-state approximation.

[1] W. Steenbock and H. Holweger, Astron. Astrophys. **130**, 319 (1984).
[2] H. W. Drawin, Z. Phys. **211**, 404 (1968).
[3] D. Lambert, Phys. Scr. **T47**, 186 (1993).
[4] I. Fleck, J. Grosser, A. Schnecke, W. Steen, and H. Voigt, J. Phys. B **24**, 4017 (1991).
[5] A. K. Belyaev, J. Grosser, J. Hahne, and T. Menzel, Phys. Rev. A **60**, 2151 (1999).
[6] M. Born and J. R. Oppenheimer, Ann. Phys. (Leipzig) **84**, 457 (1927).
[7] A. Macias and A. Riera, Phys. Rep. **90**, 299 (1982).
[8] J. Grosser, T. Menzel, and A. K. Belyaev, Phys. Rev. A **59**, 1309 (1999).
[9] A. K. Belyaev, D. Egorova, J. Grosser, and T. Menzel, Phys. Rev. A **64**, 052701 (2001).
[10] A. K. Belyaev, A. Dalgarno, and R. McCarroll, J. Chem. Phys. **116**, 5395 (2002).
[11] L. F. Errea, C. Harel, H. Jouin, L. Mendez, B. Pons, and A. Riera, J. Phys. B **27**, 3603 (1994).
[12] C.-N. Liu, A.-T. Le, T. Morishita, B. D. Esry, and C. D. Lin, Phys. Rev. A **67**, 052705 (2003).
[13] A. Boutalib and F. X. Gadéa, J. Chem. Phys. **97**, 1144 (1992).
[14] F. X. Gadéa and A. Boutalib, J. Phys. B **26**, 61 (1993).
[15] H. Croft, A. S. Dickinson, and F. X. Gadéa, J. Phys. B **32**, 81 (1999).
[16] P. J. Bruna and S. D. Peyerimhoff, Adv. Chem. Phys. **67**, 1 (1987).
[17] N. Khelifi, B. Oujia, and F. X. Gadéa, J. Chem. Phys. **116**, 2879 (2002).
[18] MOLPRO is a package of *ab initio* programs written by H.-J. Werner and P. J. Knowles, University of Birmingham, 2000.
[19] L. Méndez, I. L. Cooper, A. S. Dickinson, O. Mó, and A. Riera, J. Phys. B **23**, 2797 (1990).
[20] L. F. Errea, L. Méndez, O. Mó, and A. Riera, J. Chem. Phys. **84**, 147 (1986).
[21] H. Croft, A. S. Dickinson, and F. X. Gadéa, Mon. Not. R. Astron. Soc. **304**, 327 (1999).
[22] B. Kaulakys, J. Phys. B **18**, L167 (1985).
[23] M. F. Mott and H. S. W. Massey, *The Theory of Atomic Collisions* (Clarendon, Oxford, 1949).
[24] E. E. Nikitin, in *Atomic, Molecular, and Optical Physics Handbook*, edited by G. W. F. Drake (AIP Press, New York, 1996), Chap. 47.
[25] A. K. Belyaev and S. I. Tserkovnyi, Opt. Spectrosc. **63**, 569 (1987).
[26] A. K. Belyaev, Phys. Rev. A **48**, 4299 (1993).
[27] B. H. Bransden and C. J. Joachain, *Physics of Atoms and Molecules* (Longman, Harlow, 1983).